Examining the effect of a binding-energy-dependent clusterization algorithm on isospin-sensitive observables in heavy-ion collisions

Sanjeev Kumar[1,*] and Y. G. Ma[2,†]

[1]*Physics and Ballistics Division, State Forensic Science Laboratory, Himachal Pradesh, Shimla Hills, Junga 171218, India*

[2]*Shanghai Institute of Applied Physics, Chinese Academy of Sciences, Jiading Campus, Shanghai 201800, China*

(Received 23 June 2014; revised manuscript received 30 December 2014; published 23 March 2015)

The phase space obtained using the isospin quantum molecular dynamical (IQMD) model is analyzed by applying the binding energy cut in the most commonly and widely used secondary cluster recognition algorithm. In addition, for the present study, the energy contribution from momentum-dependent and symmetry potentials is also included during the calculation of total binding energy, which was absent in clusterization algorithms used earlier. The stability of fragments and isospin effects are explored by using the new clusterization algorithm. The findings are summarized as follows: (1) The clusterization algorithm identifies the fragments at quite early time. (2) It is more sensitive for free nucleons and light charged particles compared to intermediate mass fragments, which results in the enhanced (reduced) production of free nucleons (light charged particles, or LCPs). (3) It has affected the yield of isospin-sensitive observables—neutrons (n), protons (p), ^{3}H, ^{3}He, and the single ratio [$R(n/p)$]—to a greater extent in the mid-rapidity and low kinetic energy region. In conclusion, the inclusion of the binding energy cut in the clusterization algorithm is found to play a crucial role in the study of isospin physics. This study will give another direction for the determination of symmetry energy in heavy-ion collisions at intermediate energies.

DOI: 10.1103/PhysRevC.91.034612 PACS number(s): 25.70.Mn, 21.65.Ef, 24.10.Lx, 25.70.Pq

I. INTRODUCTION

The isospin effects in intermediate energy heavy-ion collisions have been of unique interest in the last decade. The main motive of this detailed analysis is to get rich information about symmetry energy and isospin-dependent nucleon-nucleon (NN) cross sections, or in other terms determination of the nuclear equation of state (NEOS) of asymmetric nuclear matter by studying the phenomena of multifragmentation and collective flow [1–17]. In addition, the symmetry energy and isospin-dependent cross sections play an important role in understanding many astrophysical and nuclear processes linked with neutron stars, cooling processes at critical density, as well as the liquid-gas phase transition [2,18]. A couple of sophisticated experiments have been performed to look for the isospin effects, especially in terms of symmetry energy, and many more are in progress [4,6,8,10,14,17]. Progress is also occurring on the theoretical front [1–3,5,9,11–13,15,16,19,20].

On the theoretical front, dynamical models such as the quantum molecular dynamical (QMD) [21–23] and Boltzmann-Uehling-Uhlenbeck (BUU) models [2] are used for the study of heavy-ion collisions at intermediate energies. No dynamical model simulates the fragments. Only the phase space of nucleons is obtained from the dynamical models, and fragments are supposed to be constructed by using the secondary algorithms. In the efforts to reproduce the experimental data, many secondary algorithms have been developed over time.

The most commonly used algorithm depends on the spatial and momentum coordinates of the nucleons; it is known as the minimum spanning tree (MST) algorithm [7,13,22]. According to this method, two nucleons will undergo the cluster formation if the relative distance ($|R_i - R_j|$) and relative momentum ($|P_i - P_j|$) between the nucleons are less than 3.5–4 fm and 250–268 MeV/c, respectively. These parameters can be obtained by fitting the experimental data for some of the global observables such as multiplicity of intermediate mass fragments (N_{IMFs}) [22,24]. Recently, the MST method has been further extended to isospin MST, in which the cut on the momentum space is kept thesame, bu, the cut on the spatial coordinates is constrained on the basis of type of particles. The distance between the different kinds of particles is taken as follow: $|R_i^p - R_j^p| \approx 3$ fm, $|R_i^n - R_j^p| = |R_i^n - R_j^n| \approx 6$ fm [25], where p, n stand for protons and neutrons.

The MST method has been quite successful in explaining certain fragmentation observables such as charge distribution of emitted fragments [22,26] and single and double yield ratios of neutrons to protons [6,7], while it fails to describe some important details in the production of free nucleons and light and heavy charged particles [22,26–28]. The failure results are summarized as follows: (1) The yield of $Z = 1$ is overestimated, while $Z = 2$ is underestimated. (2) In isoscaling phenomena, is there enhanced production of neutron-rich isotopes [29]? (3) Are there neutron-rich light charged particles at mid-rapidity [30]? (4) What is the behavior of Z_{bound} dependence of IMFs at high incident energy of 600 to 1000 MeV/nucleon [26,28]? The studies in the literature shows that these results cannot simply be reproduced by changing the mean field or NN cross sections in the transport model, keeping the secondary algorithm the same.

Since the MST method only depends on the constraints of position and momentum, we must consider the stability of fragments due to the formation of artificial weakly bound fragments. To avoid this problem, more complicated methods

*Author to whom all correspondence should be addressed: Sanjeev1283@gmail.com

†ygma@sinap.ac.cn

such as the stimulated annealing clusterization algorithm (SACA) [23] and the early cluster recognition algorithm (ECRA) [31] were developed. These method were found to be quite successful, but very complicated. Moreover, the choice of parameters—such as cooling parameters, iterations procedure, and choice of minima—can result in totally different configuration of fragments. Due to the limitation of sharp minima, in mildly excited or asymmetric systems, the scope of these two methods was found to be restricted at some point. The best method for avoiding the artificial formation of fragments was found to be constraining the fragments by using an average binding energy cut of -4 MeV/nucleon [26]. One can further improve the method by using the realistic binding energy cut rather than -4 MeV/nucleon [26]. This method was found to be as simple as MST and was found to reproduce the experimental data just like the complicated methods SACA, ECRA, etc.

Isospin physics, which is a new and exciting field in the present era, has been widely explored by using the simple MST method through 2013 [3,7,8,13,21]. Meanwhile, in 2012, attempts were made by incorporating modifications in MST in terms of the spatial distance between nucleons on the basis of type of particle [25]. The minimum spanning tree with binding energy check (MSTB) and other sophisticated methods in the literature were only coupled with the isospin-independent dynamical models. In these studies, MSTB, ECRA, and SACA were also found to lack the energy contribution from momentum-dependent and symmetry potentials. With the availability of an isospin-dependent version of the QMD model, it is the needed ay the present time to explore isospin physics with secondary algorithms other than simple MST and iso-MST.

In this work, for the first time, we have modified the MST method to MSTB, including the energy contribution from momentum-dependent and symmetry potentials in addition to Skyrme, Coulomb, and Yukawa interactions. The effect of MSTB is studied by considering the neutron-rich systems ^{112}Sn + ^{112}Sn and ^{124}Sn + ^{124}Sn for the yields and single ratios of isospin-sensitive particles such as n, p, ^{3}H, and ^{3}He.

The article is organized as follow: A short description of the IQMD model coupled with the secondary algorithm MSTB is given in Sec. II. The results and discussion are presented in Sec. III, followed by the conclusions in Sec. IV.

II. THE FORMALISM

A. Isospin quantum molecular dynamics (IQMD) model

In the present work, the IQMD model is used for generating the phase space of nucleons [7,13,21]. The model is modified by the authors for the density dependence of the symmetry energy, having the form

$$E_{\rm Sym}(\rho) = E^{\rm Kin}_{\rm Sym} + E^{\rm Pot}_{\rm Sym},$$

$$E_{\rm Sym}(\rho) = \frac{C_{s,k}}{2}\left(\frac{\rho}{\rho_0}\right)^{2/3} + \frac{C_{s,p}}{2}\left(\frac{\rho}{\rho_0}\right)^{\gamma_i}.$$

$E^{\rm Kin}_{\rm Sym}$ and $E^{\rm Pot}_{\rm Sym}$ are the symmetry kinetic energy and symmetry potential energy. The values of parameters $C_{s,k}$ and $C_{s,p}$ are 25 and 35.2 MeV, respectively. When we set $\gamma_i = 0.5$ and 1.5, respectively, it corresponds to the soft and stiff symmetry energies [7].

The total interaction potential is composed of Coulomb ($V_{\rm Coul}$), Yukawa ($V_{\rm Yukawa}$), local ($V_{\rm loc}$), and momentum-dependent interactions ($V_{\rm MDI}$). The expressions for $V_{\rm Coul}$ and $V_{\rm Yukawa}$ have been derived by us and others [21]. The local interaction potential $V_{\rm loc}$ originates from the Skyrme energy density function. On the basis of this, the local potential energy density is expanded as

$$U_{\rm loc} = \frac{\alpha}{2}\frac{\rho^2}{\rho_0} + \frac{\beta}{\gamma+1}\frac{\rho^{\gamma+1}}{\rho_0^{\gamma}} + E^{\rm pot}_{\rm Sym}(\rho)\rho\delta^2, \qquad (1)$$

where α, β, and γ are the parametrized values to specify the particular NEOS. A detailed table of the values is presented in Refs. [21,22].

The momentum-dependent potential has been implemented from Ref. [22] and is expressed as $V_{\rm MDI} = C_{\rm mom}\ln^2[\epsilon(\Delta p)^2 + 1]\frac{\rho}{\rho_0}\delta(r'-r)$. Here $C_{\rm mom} = 1.57$ MeV and $\epsilon = 5\times10^{-4}\frac{c^2}{MeV^2}$. The momentum is given in units of MeV/c.

Finally, combining all the potentials, we get an isospin-, density-, and momentum-dependent single-particle potential in nuclear matter, which is written as

$$V_\tau(\rho,\delta,p) = \alpha\left(\frac{\rho}{\rho_0}\right) + \beta\left(\frac{\rho}{\rho_0}\right)^{\gamma} + E^{\rm pot}_{\rm Sym}(\rho)\delta^2 + \frac{\partial E^{\rm pot}_{\rm Sym}(\rho)}{\partial\rho}\rho\delta^2 + E^{\rm pot}_{\rm Sym}(\rho)\rho\frac{\partial\delta^2}{\partial\rho_{\tau,\tau'}} + C_{\rm mom}\ln^2[\epsilon(\Delta p)^2+1]\frac{\rho}{\rho_0}. \qquad (2)$$

Here $\tau \neq \tau'$, $\frac{\partial\delta^2}{\partial\rho_n} = \frac{4\delta\rho_p}{\rho^2}$, and $\frac{\partial\delta^2}{\partial\rho_p} = \frac{-4\delta\rho_n}{\rho^2}$.

In the present simulations, the parameters α, β, and γ are -390, 320 MeV and 1.14, respectively. Moreover, the isospin- and energy-dependent NN cross section in the collision term and the quantum feature in terms of Pauli blocking are implemented.

The improved QMD (ImQMD) model, which is used in Refs. [6,25] and our IQMD model are based on the similar basic theory of the QMD model developed by Aichelin in 1991 [22]. During the modification of QMD to ImQMD and IQMD some differences are observed in terms of the Yukawa potential form, system-mass-dependent Gaussian width, symmetry energy dependent (ImQMD)/independent (IQMD) momentum dependent interactions, and shell correction factor. Due to the difference in the two models on the basis of above mentioned factors, the partial difference can be seen in the results [7].

B. Minimum spanning tree method with binding energy check (MSTB)

This method is a modified version of the normal MST and old MSTB methods. The difference between old MSTB and this MSTB is the additional contribution of energy from momentumdependent interactions and symmetry potentials in the calculation of total binding energy. The procedure is as follow: The phase space obtained from IQMD is analyzed

with the simple MST method and preclusters are sorted out. We are not knowledgable the stability of preclusters formed at this stage. So, the preclusters formed from simple MST are now subjected to the binding energy condition as follows:

$$\zeta = \frac{1}{N_f}\sum_{\alpha=1}^{N_f}\left[\sqrt{\left(\mathbf{p}_\alpha - \mathbf{P}_{N_f}\right)^2 + m_\alpha^2} - m_\alpha + \frac{1}{2}\sum_{\beta\neq\alpha}^{N_f} V_{\alpha\beta}\right], \tag{3}$$

$$\zeta < -E_{\text{bind}}. \tag{4}$$

Here, we take $E_{\text{bind}} = 4.0$ MeV/nucleon if $N_f \geqslant 3$ and $E_{\text{bind}} = 0$ otherwise. In this equation, N_f is the number of nucleons in a fragment and P_{N_f} is the average momentum of the nucleons bound in the fragment. The requirement of a minimum binding energy excludes loosely bound fragments which will decay later. The realistic value of E_{bind} changes slightly the fragment multiplicity at intermediate times, but has no influence on the quantitative behavior and on the asymptotic results. However, if by using the realistic binding energy one searches for the most bound configuration, the results are found to be affected. At the present time, we have just focused on the bound configurations and hence the average cut of binding energy −4 MeV/nucleon is justified.

If any precluster fails to meet the binding energy condition in Eqs. (3) and (4), that precluster is treated as unbound and all the nucleons of such type of precluster are treated as free nucleons. Naturally, the artificially or locally bounded fragments will be automatically discarded in the new MSTB method.

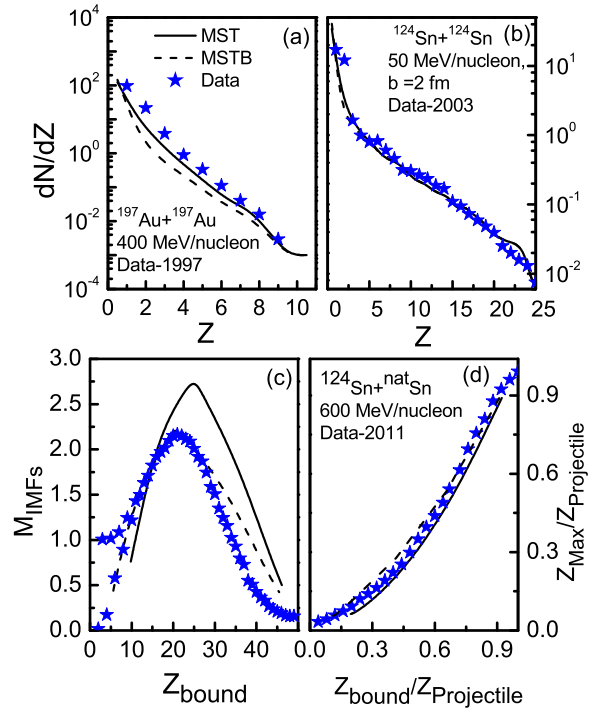

FIG. 1. (Color online) Upper panels: Comparison of charge distribution of experimental data of $^{197}\text{Au} + ^{197}\text{Au}$ and $^{129}\text{Xe} + ^{\text{nat}}\text{Sn}$ with the results obtained using MST and MSTB algorithms. Here the theoretical calculations are of $^{124}\text{Sn} + ^{124}\text{Sn}$ for the right panel. Bottom left (right) panels: Comparison of the results of $Z_{\text{bound}}(Z_{\text{bound}}/Z_{\text{projectile}})$ dependence of $M_{\text{IMFs}}(Z_{\text{Max}}/Z_{\text{projectile}})$ with the experimental data of GSI for the projectile fragmentation of ^{124}Sn.

III. RESULTS AND DISCUSSION

For the present study, thousands of events of $^{112}\text{Sn} + ^{112}\text{Sn}$ and $^{124}\text{Sn} + ^{124}\text{Sn}$ at central impact parameter between the incident energies 50 and 600 MeV/nucleon are simulated using the IQMD model coupled with MST and MSTB algorithms. For the preliminary comparison of theoretical calculations with experimental data the reactions of $^{197}\text{Au} + ^{197}\text{Au}$ (at 400 MeV/nucleon for central collisions) [32] and $^{124}\text{Sn} + ^{\text{nat}}\text{Sn}$ (at 600 MeV/nucleon throughout the collision geometry) [33] are also simulated. By checking the validity of MSTB through the comparison of our results with experimental data, the detailed analysis of rapidity and kinetic energy spectra of isospin sensitive particles such as neutrons (n), protons (p), triton (^{3}H), and helium (^{3}He) are presented.

In Fig. 1, the comparison of experimental data of charge distribution and the Z_{bound} dependence of multiplicity of intermediate mass fragments (M_{IMFs}) and Z_{Max} with the calculations of MST and MSTB algorithm is displayed. The charge distribution is displayed for $^{197}\text{Au} + ^{197}\text{Au}$ at 400 MeV/nucleon [32] (left upper panel) and $^{124}\text{Sn} + ^{124}\text{Sn}$ at 50 MeV/nucleon (right upper panel) [34]. The charge distribution at 50 MeV/nucleon is well reproduced by MST as well as MSTB algorithms, while at 400 MeV/nucleon the data is a little underestimated by MSTB. This is not surprising since it is well known that the MSTB method cannot create additional fragments; rather, it refines the fragments and hence results are logically true. Furthermore, when the recent available experimental data of Z_{bound} dependence of M_{IMFs} and Z_{max} is compared with MST and MSTB calculations, the importance of MSTB is clearly visible. In our recent communication [13], the hard equation of state with MST reproduces the data, and can be discarded on the basis of present results. The present results clearly indicate that the soft equation of state with the MSTB method can reproduce the experimental data. The results obtained are as reliable as those obtained by SACA in the previous studies [35]. This is also true for the Z_{bound} dependence of Z_{Max}. From the comparison, one can say that, except for the adjustment of mean field and collision parts in terms of the soft and hard equations of state, it is important to develop some secondary algorithms for the proper understanding of nuclear physics phenomena and the nuclear equation of state.

In Fig. 2, the time evolution of free particles, LCPs, and IMFs for neutron-poor and neutron-rich reaction system at 50 MeV/nucleon with MST and MSTB algorithms is displayed. In the high density phase, the MSTB algorithm does not find any fragment with reasonable binding energy and hence most of the particles are free, while there were a lot of artificial fragments with MST. After the high density phase is over, it starts recognizing the fragments, which are real, bound, and stable. In all the cases, MSTB helps to identify the fragments quite early. From the figure, it is clear that

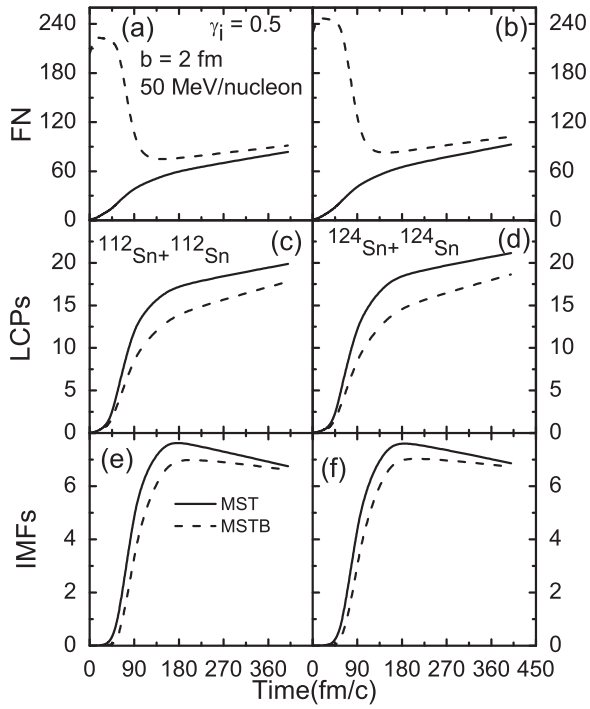

FIG. 2. The time evolution of different kinds of fragments: free nucleons (upper), LCPs (middle), and IMFs (bottom) for central collisions at 50 MeV/nucleon with MST and MSTB algorithms. The left (right) panels are for neutron-poor (neutron-rich) ^{112}Sn + ^{112}Sn (^{124}Sn + ^{124}Sn) reaction systems. All the results are with soft symmetry energy.

MSTB enhances the production of free particles and reduces the production of LCPs and IMFs. Moreover, with increase in the size of the fragment, MST takes less time to match with the MSTB results and also the difference between MST and MSTB results goes on decreasing throughout the time evolution.

During the comparison of results between neutron-poor and neutron-rich reaction systems, it is found that enhanced production of fragments takes place for the more neutron-rich system. The enhanced production is sensitive for free nucleons and LCPs compared to IMFs. It was also shown by us recently that free nucleons and LCPs are more sensitive to the symmetry energy compared to IMFs [13]. In this regard, the sensitivity of free nucleons and LCPs with MSTB in more neutron-rich systems can also play an important role in the prediction of symmetry energy, which is a topic of separate discussion. For further study, the isospin-sensitive free nucleons and LCPs, namely, n, p, ^{3}H, and ^{3}He are used.

In the literature, isospin effects, especially symmetry energy, have been predicted by using the rapidity and kinetic energy spectra of yield, ratio, or flow of different kinds of isobaric or isotopic particles [2,7,11]. Following the same process, in Figs. 3 (4), we display the rapidity distribution (kinetic energy spectra) of isospin sensitive particles n, p, ^{3}H, and ^{3}He with MST and MSTB algorithms for neutron-poor as well as neutron-rich reaction systems. In addition, the differential distribution is also plotted in the extreme right panel of both the figures. In Fig. 3, with the increase in isospin of the system, the results with MSTB (MST) affect the yield of neutron-rich (proton rich) particles, i.e., neutrons and ^{3}H (protons and ^{3}He) over all the rapidity region, especially at mid-rapidity. This indicates the weak (strong) contribution of Coulomb effects (symmetry energy) with MSTB compared to MST. These finding strengthen MSTB as a good method for better understanding the symmetry energy.

The clear isospin effects can be seen from the differential rapidity distribution of (n-p) and (^{3}H-^{3}He). For neutron-rich systems, quite strong sensitivity can be seen of the differential distribution compared to the individual yield distribution with MSTB. This is true for the (n-p) as well as (^{3}H-^{3}He) differential rapidity distributions.

Let us move toward discussing the kinetic energy distribution (Fig. 4). The sensitivity to the method of clusterization and isospin physics, collectively, is observed at lower end of kinetic energy spectra of neutrons and differential (n-p); however, at higher kinetic energies, spectra are only sensitive to the isospin physics and not to the method of clusterization. Due to the low yield of ^{3}H and ^{3}He particles at 50 MeV/nucleon, it is hard to identify the isospin effects. It is concluded that free neutrons' individual and n-p (^{3}H-^{3}He) differential spectra at low (high) kinetic energy as well as at mid-rapidity affect the results significantly with the MSTB method over the MST method.

In order to elaborate the kinetic energy spectra further, the kinetic energy dependence of single ratios is shown in Figs. 5 at 50 MeV/nucleon. In Fig. 5, more MSTB effects are observed for neutron-rich systems throughout the kinetic energy for the single neutrons-to-protons ratio. As discussed earlier, the sensitivity of MSTB over MST decreasing with higher kinetic energy is also true here. No systematic results are observed with the present data for ^{3}H/^{3}He. The statistics need to be improved for this in the near future. The higher single ratio with the simple MST algorithm is due to the decreased production of protons and not many neutrons for the neutron-rich system. The real strength of the symmetry energy is to enhance the production of neutrons due to the repulsive nature. The binding energy algorithm enhances (decreases) the production of neutrons (protons) to a great (weak) extent in more neutron-rich systems. The weak sensitivity of MSTB to the proton production is justified as the reaction systems ^{112}Sn and ^{124}Sn have the same number of protons and different numbers of neutrons. Including the binding energy effects strengthens proper understanding of isospin effects due to symmetry energy. One must take caution when considering the enhanced single neutrons-to-protons ratio with simple MST as a signature of symmetry energy.

For better understanding, one must check the sensitivity of the yield contribution of different particles using the linear or power-law fit method. In Fig. 6, the isospin asymmetry dependence of the yield of different particles and corresponding ratios is fitted with a power law of the form $Y = AX^{\tau}$. The numerical values in the figure show the value of the power law parameter τ. The production of neutron-rich (proton-rich) particles n, ^{3} (p, ^{3}He) is increasing (decreasing) with isospin asymmetry of the system for the MST as well as the MSTB algorithm. In comparison of neutron-rich particles, n (^{3}H)

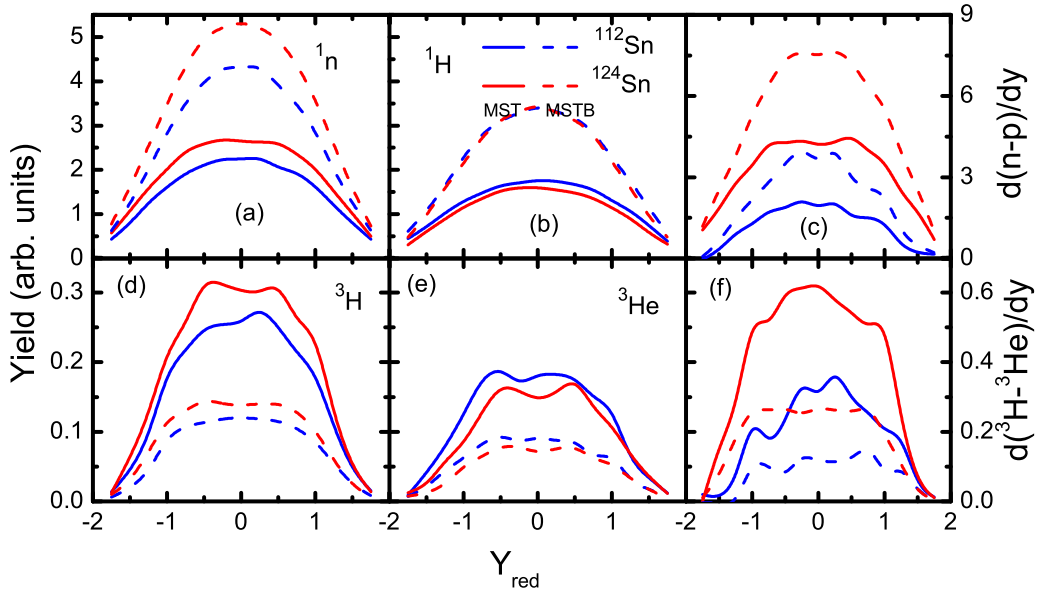

FIG. 3. (Color online) The rapidity distribution of neutrons, protons, and ^{3}H and ^{3}He particles for neutron-poor and neutron-rich reaction systems with MST and MSTB algorithms. The results for the differential rapidity distributions of (n-p) and (^{3}H -^{3}He) are also presented in the right top and bottom panels, respectively.

production is more sensitive with the MSTB (MST) algorithm; however, in comparison of proton-rich particles p (^{3}He) are more sensitive with the MST (MSTB) algorithm. This indicates that ^{3}H and ^{3}He produced with simple MST are greatly unstable. Especially, this is true for ^{3}He particles, which is already verified from the physics point of view. Furthermore, the sensitivity of the n/p (^{3}H/^{3}He) ratio is high with the MST method. Interestingly, the sensitivity parameter difference of MST over MSTB is quite strong for n/p compared to ^{3}H/^{3}He. This difference motivated us to study the same sensitivity at high incident energy.

Just like in Fig. 6, the isospin asymmetry dependences of n/p and ^{3}H/^{3}He are fitted at the high incident energies of 100, 200, 400, and 600 MeV/nucleon with the power law. The incident-energy dependence of the power law parameter τ is shown in Fig. 7. The sensitivity of n/p (^{3}H/^{3}He) decreases with higher incident energy (zigzag motion). For n/p, it is due to the importance of other degrees of freedom such as meson production and nucleon resonances at high incident energy. Up to 1 GeV/nucleon, ultrarelativistic QMD (UrQMD) [38] as well as IQMD [21] can explain the experimental GSI data with a good degree of accuracy. For better reproduction of experimental data with the IQMD model at and above 600 MeV/nucleon up to 1 GeV/nucleon, the different kinds of clusterization method also play a quite important role [26,35]. In addition, UrQMD, in which meson production and nucleon resonances are well treated, has been able to explain the experimental data above 1 GeV/nucleon also, where the

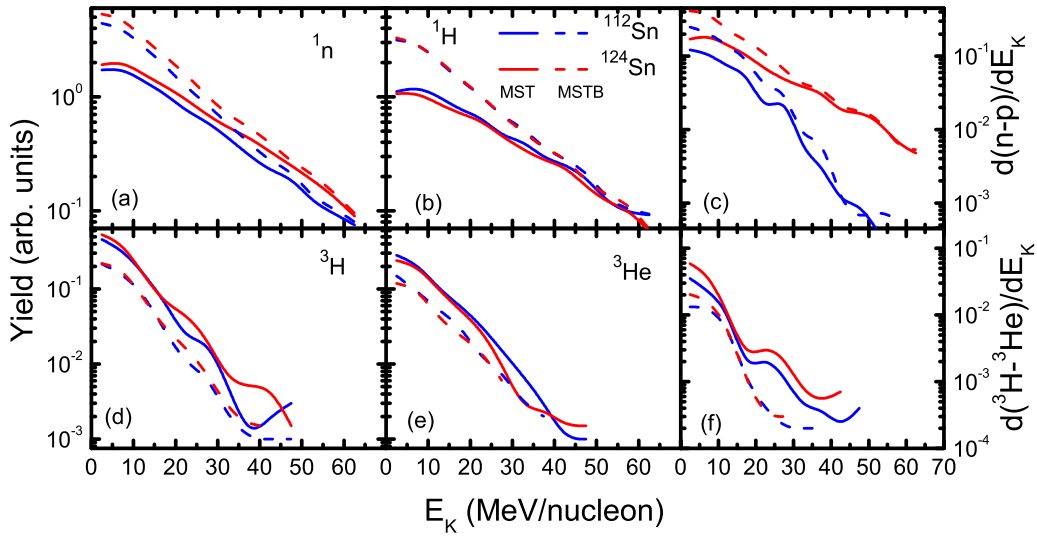

FIG. 4. (Color online) Same as in Fig. 3, but for the kinetic energy dependence instead of rapidity distribution dependence.

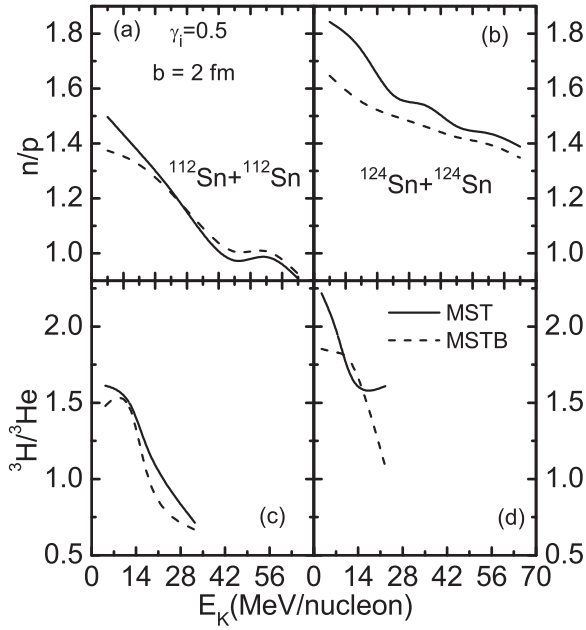

FIG. 5. The kinetic energy dependence of single n/p (^{3}H/^{3}He) in the top (bottom) panels for neutron-poor and neutron-rich reaction systems with MST and MSTB algorithms.

IQMD model fails badly. For ^{3}H/^{3}He, the zigzag behavior with incident energy is due to the plateau formation for LCP production around 400 MeV/nucleon[36]. The sensitivity of n/p (^{3}H/^{3}He) with MSTB is decreasing (increasing) with higher incident energy, which is a quite interesting observation. The study clearly indicates that the contribution of different

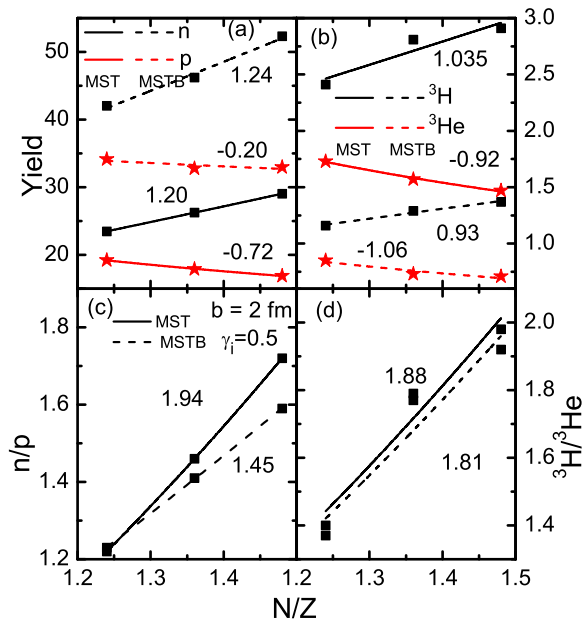

FIG. 6. (Color online) Isospin-asymmetry dependence of yield of neutrons and protons (^{3}H and ^{3}He) with MST and MSTB algorithms in the top left (right) panels. The corresponding n/p (^{3}H/^{3}He) dependence is shown in the bottom left (right) panels. All the lines are fitted with a power law of the form $Y = AX^{\tau}$.

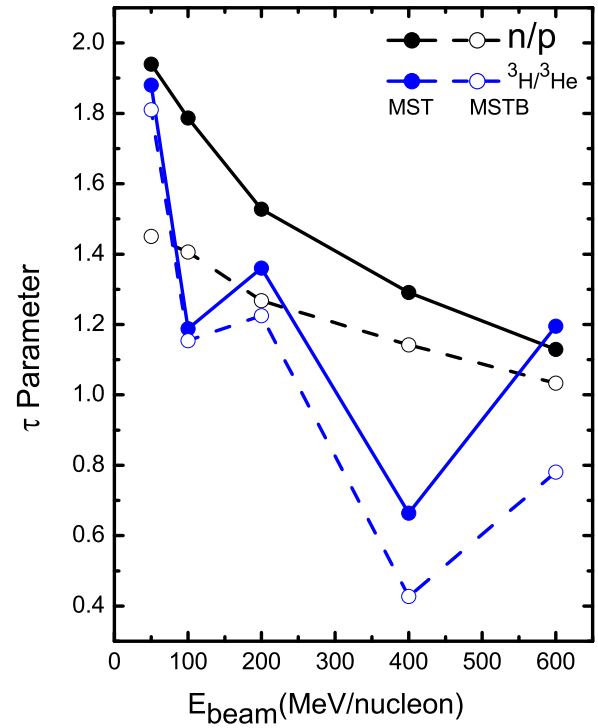

FIG. 7. (Color online) Incident energy dependences of the power-law-fitted parameter τ [from isospin asymmetry dependence of n/p and (^{3}H/^{3}He) at different incident energies] with MST and MSTB algorithms.

types of particles to the isospin physics at higher incident energies with different clusterization methods is found to vary drastically [37].

IV. CONCLUSION

In conclusion, we have introduced, for the first time, a clusterization method with binding energy cut coupled with IQMD in order to understand the isospin physics. Binding energy clusterization methods such as MSTB and SACA were used earlier for the study of many phenomena in heavy-ion collisions at intermediate energies [23,26,31,35], but not for the study of isospin physics. The importance of the present MSTB method is as follows: (1) The contribution of energy from momentum-dependent interactions and the symmetry potential is included during the calculation of the total binding energy of fragments, which affects the actual yield of fragments compared to the earlier MSTB method. (2) When the method is applied to isospin-sensitive fragments, a drastic variation in the results can be seen, which was never checked with this method earlier.

The summarized results are as follows. With this method, we found enhanced production of free nucleons, with decreased production of light charged particles. The free-nucleon enhancement is mostly found to be contributed from the symmetry-energy-sensitive particles, i.e., neutrons. The absolute and differential yields of isospin-sensitive particles—n, p, ^{3}H, and ^{3}He—are found to be greatly affected by MSTB in the mid-rapidity and low kinetic energy region. The magnitude

of the kinetic-energy dependence of the single neutrons-to-protons ratio is found to decrease with MSTB, and is mostly affected in neutron-rich systems. The yield sensitivity with the MSTB method toward higher incident energy is found to decrease (increase) for n/p (^{3}H/^{3}He). The sensitivity at high incident energy needs to be tested in the future. In conclusion, the binding energy cut is of utmost importance in heavy-ion collisions at intermediate energies in order to understand the isospin physics and stability of fragments.

ACKNOWLEDGMENTS

This work is supported in part by the Chinese Academy of Sciences Support Program for young international scientists under Grant No. 2010Y2JB02, the National Science Foundation of China under Contracts No. 11035009, No. 10979074, and No. 11421505, and the Knowledge Innovation Project of the Chinese Academy of Sciences under Grant No. KJCX2-EW-N01.

[1] S. Gautam, R. Kumari, and R. K. Puri, Phys. Rev. C **86**, 034607 (2012).
[2] B. A. Li, L. W. Chen, and C. M. Ko, Phys. Rep. **464**, 113 (2008).
[3] A. Jain, S. Kumar, and R. K. Puri, Phys. Rev. C **85**, 064608 (2012).
[4] J. B. Natowitz *et al.*, Phys. Rev. Lett. **104**, 202501 (2010); L. Qin *et al.*, *ibid.* **108**, 172701 (2012).
[5] S. Gautam, A. D. Sood, R. K. Puri, and J. Aichelin, Phys. Rev. C **83**, 034606 (2011).
[6] M. B. Tsang, Y. Zhang, P. Danielewicz, M. Famiano, Z. Li, W. G. Lynch, and A. W. Steiner, Phys. Rev. Lett. **102**, 122701 (2009); D. D. S. Coupland, W. G. Lynch, M. B. Tsang, P. Danielewicz, and Y. Zhang, Phys. Rev. C **84**, 054603 (2011).
[7] S. Kumar, Y. G. Ma, G. Q. Zhang, and C. L. Zhou, Phys. Rev. C **84**, 044620 (2011); **85**, 024620 (2012).
[8] Z. Y. Sun *et al.*, Phys. Rev. C **82**, 051603(R) (2010).
[9] Z. G. Xiao, B. A. Li, L. W. Chen, G. C. Yong, and M. Zhang, Phys. Rev. Lett. **102**, 062502 (2009).
[10] P. Russotto *et al.*, Phys. Lett. B **697**, 471 (2011).
[11] Z. Q. Feng, Phys. Lett. B **707**, 83 (2012).
[12] W. J. Xie, J. Su, Z. Zhu, and F. S. Zhang, Phys. Lett. B **718**, 1510 (2013).
[13] S. Kumar and Y. G. Ma, Nucl. Phys. A **898**, 59 (2013).
[14] M. B. Tsang *et al.*, Phys. Rev. Lett. **92**, 062701 (2004); M. A. Famiano *et al.*, *ibid.* **97**, 052701 (2006).
[15] B. A. Li, Phys. Rev. Lett. **88**, 192701 (2002).
[16] B. A. Li, L. W. Chen, H. R. Ma, J. Xu, and G. C. Yong, Phys. Rev. C **76**, 051601(R) (2007).
[17] F. Amorini *et al.*, Phys. Rev. Lett. **102**, 112701 (2009).
[18] J. M. Lattimer and M. Prakash, Science **304**, 536 (2004); D. T. Loan, N. H. Tan, D. T. Khoa, and J. Margueron, Phys. Rev. C **83**, 065809 (2011).
[19] S. S. Bao and H. Shen, Phys. Rev. C **89**, 045807 (2014).
[20] Y. Wang, C. Guo, Q. Li, H. Zhang, Y. Leifels, and W. Trautmann, Phys. Rev. C **89**, 044603 (2014).
[21] C. Hartnack *et al.*, Eur. Phys. J. A **1**, 151 (1998).
[22] J. Aichelin, Phys. Rep. **202**, 233 (1991); E. Lehmann *et al.*, Prog. Part. Nucl. Phys. **30**, 219 (1993).
[23] R. K. Puri and J. Aichelin, J. Comput. Phys. **162**, 245 (2000).
[24] J. Singh and R. K. Puri, Phys. Rev. C **62**, 054602 (2000).
[25] Y. Zhang, Z. Li, C. Zhou, and M. B. Tsang, Phys. Rev. C **85**, 051602 (2012).
[26] S. Goyal and R. K. Puri, Phys. Rev. C **83**, 047601 (2011).
[27] R. Nebauer *et al.*, Nucl. Phys. A **658**, 67 (1999).
[28] S. Kumar and S. Kumar, Pramana J. Phys. **74**, 731 (2010).
[29] T. X. Liu *et al.*, Phys. Rev. C **69**, 014603 (2004).
[30] Z. Kohley *et al.*, Phys. Rev. C **83**, 044601 (2011).
[31] C. O. Dorso and J. Randrup, Phys. Lett. B **301**, 328 (1993).
[32] W. Reisdorf *et al.*, Nucl. Phys. A **612**, 493 (1997).
[33] R. Ogul *et al.*, Phys. Rev. C **83**, 024608 (2011).
[34] S. Hudan *et al.*, Phys. Rev. C **67**, 064613 (2003).
[35] Y. K. Vermani and R. K. Puri, Europhys. Lett. **85**, 62001 (2009).
[36] S. Kumar, S. Kumar, and R. K. Puri, Phys. Rev. C **81**, 014601 (2010).
[37] S. Kumar and R. K. Puri, Phys. Rev. C **58**, 2858 (1998).
[38] Q. F. Li, Z. Li, E. Zhao, and R. K. Gupta, Phys. Rev. C **71**, 054907 (2005); H. Peterson, Q. Li, X. Zhu, and M. Bleicher, *ibid.* **74**, 064908 (2006); Y. Yuan, Q. Li, Z. Li, and F. H. Liu, *ibid.* **81**, 069901(E) (2010); Q. Li, C. Shen, C. Guo, Y. Wang, Z. Li, J. Lukasik, and W. Trautmann, *ibid.* **83**, 044617 (2011); G. Graf, M. Bleicher, and Q. Li, *ibid.* **85**, 044901 (2012).